

A VISUAL NAVIGATION SYSTEM FOR AUTONOMOUS UNDERWATER VEHICLE

Wang Jian-gang, Hao Ying-ming, Cao Hong-kai, Yu Yong,
Xu Xin-ping

Shenyang Inst. of Automation, Chinese Academy of Sciences
Robotics lab., Chinese Academy of Sciences
Shenyang 110015, P. R. China

ABSTRACT

In this paper we present a visual navigation system for retrieving untethered autonomous underwater vehicle (AUV). The vision system guides the AUV into a retriever which is a tethered underwater robot. The visual navigation modules include target searching, line tracking, and positioning. The vision system is a dedicated parallel image processor composed of three T800 (Transputer). The processing speed and positioning precision meet the needs of AUV close-loop control.

1. INTRODUCTION

The research on visual navigation used for autonomous underwater vehicle (AUV) has just begun recently. Nguyen uses Hough transformation to find the straight line in an underwater image for guiding the AUV along the cables and chains [1]. Hallset finds the underwater pipeline using image segmentation to provide navigation information [2].

In this paper we describe an unmanned untethered AUV "Explorer" that submerges 1000 meter depth working for sea floor survey.

The retrieve of AUV is a key step in entire underwater operation. Because of the limitation of sonar positioning precision, there is great location error for robot navigation. The error may be beyond 30 meters even if using the more precise ultrashort baseline sonar. Another difficulty is that in the fourth class wave scale situation, it is almost impossible to accomplish AUV retrieve. So we adopt vision system with higher positioning precision to guide the AUV autonomous retrieve underwater 50 meter depth where the sea current was steady.

This paper will describe distortion correcting and calibration algorithm for omnidirectional image first. Then mainly discuss tracking and positioning method used in robot retrieve. Finally, the vision hardware system and experiment results are given.

2. VISUAL NAVIGATION RETRIEVE

Untethered AUV retrieve will be done underwater 50 meter depth. In fact, the retriever is a tethered underwater robot (Fig. 1). The retriever is connected with vessel through the relay. The cable is about 100 meters long. The retriever have two movable arms. When the untethered AUV is guided into the retriever, the retriever's arms will close tightly. Then the retriever together with the AUV will be hauled up to the sea surface and returns to the vessel.

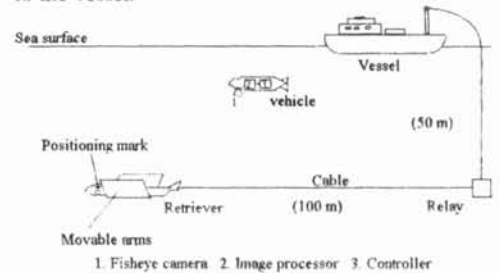


Fig. 1 Retrieve system.

For guiding the AUV into retriever, first the positioning sonar is used to guide the AUV to the area about 8 meters above the retriever and within a radius of 50 meters, Then the visual navigation system begins to work.

The algorithm of visual navigation can be divided into three modules (Fig. 2).

(1) Target searching.

In this time the AUV moves around in a variety of radius to search the target. The easiest and most reliable target to be found is the cable with thin and long straight line. When the straight line is found, it is turned to the stage of cable tracking. If the vision system finds the location mark which is two circles with different radius fixed on the head of retriever, it is shown that the AUV has moved to the area just above the retriever. Then it is directly turned to the stage of positioning.

(2). Cable tracking.

If a line is found, the location and orientation of line can be determined, and the position data are reported to the controller to guide the AUV moving to retriever along the cable.

(3). Positioning and Dropping

If circles are found, the six degrees of freedom between AUV and retriever can be determined by the

circle positioning method. This method will be described in more detail in section 5. These positioning data are reported to the controller for guiding the AUV dropping into retriever properly.

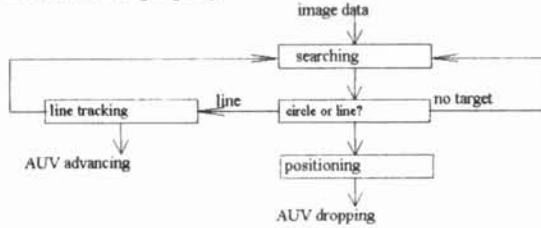


Fig. 2 Visual navigation retrieve modules

3. DISTORTION CORRECTING AND CALIBRATION OF OMNI-DIRECTIONAL IMAGE

The vision system uses a omnidirectional camera to acquire the underwater image, because this camera has super wide-angle lens (fish-eye lens) and can get large field of view for target searching. The omnidirectional image model is not similar to the pin hole model. The image has larger geometric distortion. The previous research on distortion correcting was concentrated on the methods of using spherical model that is not satisfied for use in water.

We use a polynomial expression

$$x = \sum_{i=0}^N \sum_{j=0}^N a_{ij} u^i v^j, \quad y = \sum_{i=0}^N \sum_{j=0}^N b_{ij} u^i v^j \quad (1)$$

to describe the relationship of omnidirectional model and pin hole model. The omnidirectional image then can be transformed to pin hole image and the common camera calibration method [3][4] can be used to calibrate omnidirectional image. The problem of the method is large computation cost. We develop a fast algorithm which divides the whole image into some small images, and use lower order polynomial instead of higher order one. Only limited points of image are calculated by polynomial. Another advantage of this method is that it can only use small memory and it is easy to control the field of view. The result is shown as figure 3.

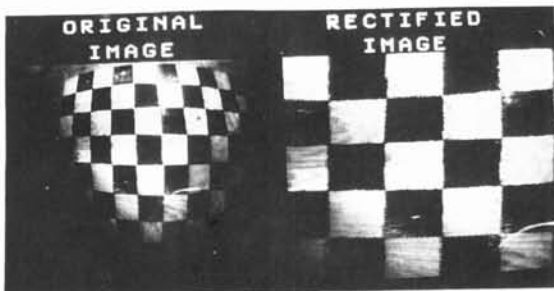


Fig. 3. The origin and rectified image

We develop a method to calibrate the distortion image that concern with tangential distortion.

$$\begin{aligned} \delta_u &= k_1 u + k_2 u(u^2 + v^2) + O[k_3(u, v)^5] \\ \delta_v &= k_1 v + k_2 v(u^2 + v^2) + O[k_3(u, v)^5] \end{aligned} \quad (2)$$

where k_1, k_2, k_3 are distortion parameter.

4. CABLE TRACKING

(1). Straight line fitting

The automatic thresholding method is used to detect the feature points of cable line from background. The 4-connected neighbors region tracking algorithm is used for region segmentation. Using the least-squares error fitting method, we can identify the straight line.

For example, supposing the line equation is

$$y = ax + b.$$

Using the least-squares fitting method, we can obtain

$$\begin{aligned} a &= \frac{\sum_{i=1}^n x_i y_i - n \bar{x} \bar{y}}{\sum_{i=1}^n x_i^2 - n \bar{x}^2} \\ b &= \bar{y} - a \bar{x} \end{aligned} \quad (3)$$

where $\bar{x} = \frac{\sum_{i=1}^n x_i}{n}, \quad \bar{y} = \frac{\sum_{i=1}^n y_i}{n}$

(2). cable tracking

The depth of the retriever and the AUV can all be measured out from sonar sensor. So the height from retriever to the AUV is given. The angle θ between the AUV and cable and the intercept b' of the line in AUV coordinate system can be found from following formula.

$$\theta = \arctan(a), \quad b' = \frac{b}{f} \cdot h \quad (4)$$

where f is the camera focal length.

The results of θ and b' are sent to the AUV controller to guide it moving to the retriever along the cable.

5. POSITIONING

We develop a monocular camera positioning method based on two circles in the same plane.

(1). Ellipse fitting

The circle's trace is a ellipse in image plane, so we do ellipse fitting with the detected feature points in the positioning stage first.

Supposing the ellipse equation is

$$x^2 + ay^2 + bxy + dx + ey + c = 0 \quad (5)$$

Using the least-squares fitting method we can calculate the values of a, b, c, d, e from the detected points in the ellipse.

Normalizing the equation (5), we can obtain the major and minor axis of the ellipse.

(2). Positioning

The spacial relation of a circle in 3D space and the image plane is shown in Fig. 4.

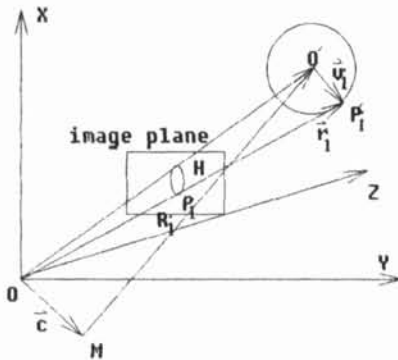


Fig. 4 The spacial relation of a circle and the image plane

The camera coordinate system is O-XYZ, the circle center is O' and the radius is k. p_i' is a point in the circle, p_i is its projection point in image plane. The circle's perspective in image plane is ellipse H. It can be thought that a circle is a trace of spacial point moving around a axis in three dimension shown as figure 4.

- \hat{b} : unit vector in same direction of rotational axis
- \hat{c} : the vector through the origin and perpendicular to \hat{b}
- d: the distance from point M to O'
- \vec{r}_i : the spacial vector of a point p_i' on the circle.
- \vec{R}_i : the spacial vector of p_i
- \vec{v}_i : the vector from circle center to a point p_i'
- f: camera focal length.

From Fig. 4, we can obtain the expression of ellipse H.

$$\vec{R}_i^T [d^2[I] - d[\hat{c}\hat{b}^T + \hat{b}\hat{c}^T] + \tau_c[\hat{b}\hat{b}^T]] \vec{R}_i = 0 \quad (6)$$

$$\text{where } \tau_c = \hat{c}^T \hat{c} - d^2 - k^2$$

Defining

$$[Mexp] = [d^2[I] - d[\hat{c}\hat{b}^T + \hat{b}\hat{c}^T] + \tau_c[\hat{b}\hat{b}^T]] \quad (7)$$

The circle project equation in image plane can be determined by the matrix [Mexp].

Let $|\hat{c}|=1$, [Mexp] can be normalized by $|\hat{c}|$.

$$[Mexp] = [d^2[I] - d[\hat{c}\hat{b}^T + \hat{b}\hat{c}^T] + \tau_i[\hat{b}\hat{b}^T]] \quad (8)$$

$$\text{where } \tau_i = 1 - d^2 - k^2$$

By choosing the coordinaion system, \hat{b} , \hat{c} can be expressed in the form of [0,0,1] and [0,1,0], then [Mexp] have three characteristic values

$$\lambda_1 = d^2 \quad (9)$$

$$\lambda_2 = \frac{1}{2} (\tau_2 + \sqrt{\tau_2^2 - 4d^2k^2}) \quad (10)$$

$$\lambda_3 = \frac{1}{2} (\tau_2 - \sqrt{\tau_2^2 - 4d^2k^2}) \quad (11)$$

$$\text{where } \tau_2 = 1 + d^2 - k^2$$

Because of the coordination system do not change the characteristic values of [Mexp], so the characteristic value of [Mexp] is still $\lambda_1, \lambda_2, \lambda_3$ in original camera coordinate system. Where $\lambda_1 > 0$, $\lambda_2 > 0$, and $\lambda_1 \leq \lambda_2$, $\lambda_3 < 0$.

Suppose [Mcom] is the symmetric matrix of homogenous coordinate equation for a ellipse fitted from practical image plane by the least-squared method.

The characteristic values of [Mexp] are r_1', r_2', r_3' , $r_1' \leq r_2'$ and $r_1' > 0$, $r_2' > 0$, $r_3' < 0$. If $r_1' = r_2'$, then rotating axis pass throught the origin O and the direction of the characteristic vector \vec{r}_3 in correspondence with r_3' is the same with \hat{b} . Otherwish $r_1' < r_2'$, because it is just different with a same coefficient δ between r_1', r_2', r_3' and $\lambda_1, \lambda_2, \lambda_3$, let

$$\lambda_1 = \frac{r_1'}{\delta}, \quad \lambda_2 = \frac{r_2'}{\delta}, \quad \lambda_3 = \frac{r_3'}{\delta}$$

From [9]-[11], we have

$$\begin{aligned} \lambda_2 + \lambda_3 &= \frac{r_2'}{\delta} + \frac{r_3'}{\delta} = \tau_2 = 1 + d^2 - k^2 \\ \lambda_2 \cdot \lambda_3 &= \frac{r_2'}{z} \cdot \frac{r_3'}{z} = -d^2k^2 \\ \lambda_1 &= \frac{r_1'}{z} = d^2 \end{aligned} \quad (12)$$

$$d^2 = \frac{1}{r_1 + r_2 - r_1 r_2 - 1}$$

$$\text{where } k^2 = -r_1 r_2 d^2$$

$$r_1 = \frac{r_2'}{r_1'} \quad r_2 = \frac{r_3'}{r_1'}$$

Let \hat{n}_1 is the normal line of the plane \hat{b}, \hat{c} , then \hat{n}_1 satified $[Mexp] \hat{n}_2 = d^2 \hat{n}_1 = \lambda_1 \hat{n}_1$. It is shown that \hat{n}_1 is a charactric vector in correspondence with λ_1 , other two charactric vectors \hat{n}_2, \hat{n}_3 of charactric value λ_2, λ_3 must be in the plane \hat{b}, \hat{c} , then

$$\begin{aligned} \hat{c} &= \cos \theta \cdot \hat{n}_2 - \sin \theta \cdot \hat{n}_3 \\ \hat{b} &= \sin \theta \cdot \hat{n}_2 + \cos \theta \cdot \hat{n}_3 \end{aligned} \quad (13)$$

From [13] and [7], and as

$$[M \exp] \hat{n}_2 = \lambda_2 \hat{n}_2$$

$$[M \exp] \hat{n}_3 = \lambda_3 \hat{n}_3$$

we obtain

$$\tan \theta = \frac{d^2 - \lambda_2}{d}$$

Therefore \hat{b}, \hat{c} can be solved from [13]. For the object before the camera, the Z axis direction of \hat{b} is always positive. so \hat{b}, \hat{c} have two different groups of solution. By the consistency constraint of the normal direction for two different circles in the same plane, we can remove a group of solution and find a unique solution of rotating axis \hat{b} .

Under the condition of $|\hat{c}| = 1$, we have solved \hat{b}, \hat{c}, d, k , then the corresponding OO' vector is $\overline{oo'} = \hat{c} + \hat{b} \cdot d$. Given the circle radius R_s , the scale factor for the

$d, k, \hat{c}, \overline{oo'}$ can be defined uniquely $\Delta = \frac{R_s}{k}$. The position of circle center is $\overline{oo'} \cdot \Delta$.

In the left hand coordination system, the vector from big circle to small one is X axis and plane normal vector \hat{b} is Z axis, we can define the Y axis uniquely. Then we can derive the spacial relation between the camera coordination system and above coordination system, the six degrees of freedom.

6. EXPERIMENT RESULTS AND CONCLUSIONS

We have developed a dedicated parallel image processing system which was built by Transputer network. The system includes a single-board frame grabber with a T800 (IFG) which receives the input from an omnidirectional camera, a Transputer accelerator board (MTM) that have two T800, and an all-in-one PC CPU board with electronic solid state disk (Fig. 5). The visual navigation algorithms are implemented using OCCAM, the dedicated language of transputer. All procedures are parallelly run in the system.

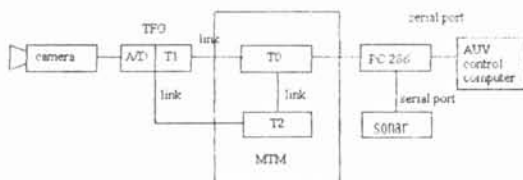


Fig. 5 The configuration of visual navigation system

The experiment is conducted in underwater laboratory. Fig. 6 is the image of retriever with cable and two circle mark picked from the camera under water. Table 1 shows the processing time and tracking errors. The real height of camera from retriever is 5.0m and the distance of circle centers is 80.0 cm.

Table 1 Average computation Time and Error.

cable tracking	processing time (sec)	angle error (degree)	intercept error(cm)
	0.11	2.00	4.90
circle positioning	processing time (sec)	depth (cm)	distance of circle centers(cm)
	0.18	488.00	79.80

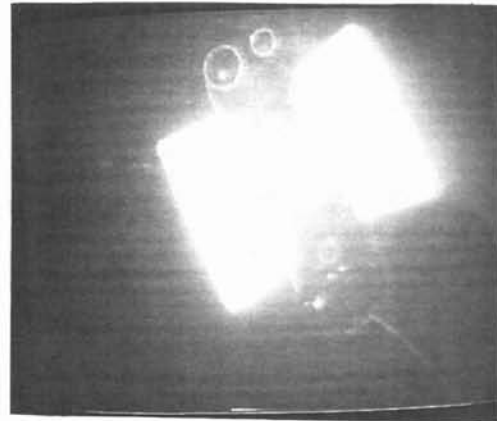


Fig. 6 Robot retriever with cable and two circle marks.

The experiment results show that the visual navigation system has good navigation precision and robustness. The processing times in different stages successfully meet the needs for close-loop control of AUV.

REFERENCE

1. H. G. Nguyen, P. J. Heckman, A. L. Pai, Real Time Pattern Recognition for Guidance of an Autonomous Undersea Submersible, Proc. of IEEE Conf. on Robotics and Automation, 1988, pp1767-1770
2. J. O. Hallset, Simple Vision Tracking of Pipeline for Autonomous Underwater Vehicle, Proc. of the IEEE International Conf. on Robotics and Automation, 1991, pp2767-2772
3. S. Ganapathy, Decomposition of Transformation Matrices for Robot Vision, Pattern Recognition Letters 2, 1984, pp401-412
4. J. Weng, P. Cohen, M. Herniou, Camera Calibration with Distortion Models and Accuracy Evaluation, IEEE trans. on PAMI 14(10), 1992, pp965-980
5. Raze Safaee-Rad, Ivo tchoukanov, Kemeth Carless Smith, Bensiyon Benhabib, Three-Dimensional Location Estimation of Circular Features for Machine Vision, IEEE trans. on Robotics and Automation, Vol. 8, No. 5, Oct., 1992, pp624-639